DFT Study of the Structure and Spectral Behavior of New Pt(II) Complexes With 5-Methyl-5(4-pyridyl)hydantoin

5 AUTHORS, INCLUDING:

Adriana Bakalova
Medical University of Sofia
28 PUBLICATIONS **187** CITATIONS

SEE PROFILE

Hristo Plamenov Varbanov
Ecole polytechnique fédérale de Lausanne,…
18 PUBLICATIONS **145** CITATIONS

SEE PROFILE

Stancho Stanchev
Academy of Sciences of the Czech Republic
19 PUBLICATIONS **139** CITATIONS

SEE PROFILE

Frank Jensen
Aarhus University
153 PUBLICATIONS **6,206** CITATIONS

SEE PROFILE

DFT Study of the Structure and Spectral Behavior of New Pt(II) Complexes With 5-Methyl-5(4-pyridyl)hydantoin

ADRIANA BAKALOVA,[1] HRISTO VARBANOV,[1] STANCHO STANCHEV,[2] DARVIN IVANOV,[1] FRANK JENSEN[3]

[1]Department of Chemistry, Faculty of Pharmacy, Medical University - Sofia, 2 Dunav St., 1000 Sofia, Bulgaria

[2]Department of Organic Chemistry, Faculty of Pharmacy, Medical University - Sofia, 2 Dunav St., 1000 Sofia, Bulgaria

[3]Department of Chemistry, Faculty of Science, University of Aarhus, Langelandsgade 140, DK-8000 Aarhus C, Denmark

ABSTRACT: Platinum complexes are a great interest of study, because of the antitumor activity and the clinical use of some of them in the recent anticancer chemotherapy. In many cases, computational studies can be very useful for predicting the structure and some physicochemical properties of metal complexes. Theoretical calculations can also be used for the rational design of new complexes with optimal ratio: antitumor activity/toxicity. The geometry of three new Pt(II) complexes with general formula cis-[PtL$_2$X$_2$] (where L is 5-methyl-5(4-pyridyl)hydantoin and X = Cl$^-$, Br$^-$, I$^-$) and of the free organic ligand were optimized using the hybrid DFT method B3LYP with LAN2DZ basis sets. The results were in very good correlation with the data of similar compounds from the literature. The same DFT method was used for the study of their spectral behavior, by reproducing their IR and Raman spectra and comparing them with experimental data. In addition, the distribution of charges by ESP analysis was calculated.   © 2008 Wiley Periodicals, Inc. Int J Quantum Chem 109: 826–836, 2009

Key words: Pt(II) complexes; hydantoins; DFT study; IR spectra; Raman spectra

Correspondence to: A. Bakalova; e-mail: adrigebk@abv.bg

Introduction

After the discovery of cell division inhibiting effect of cisplatin by Rosenberg et al. [1], there is considerable interest in platinum chemistry. Lately, six platinum complexes (including cisplatin) are used in the recent anticancer chemotherapy [2].

Many computing investigations of the molecular structure and properties of platinum-based drugs were carried out. Density functional theory (DFT) methods in comparison with HF, MP2, MP3, and MP4 were used in the investigation of the conformational and vibrational behavior of cisplatin [3, 4].

The molecular structure, vibrational frequencies, IR intensities, and Raman scattering activities were recently calculated for carboplatin, using DFT methods. Best results were obtained with the mPW/LanL2DZ level of theory [5]. Recently, the structure and chemical reactivity of some selected *cis*-platinum(II) complexes, including clinically used drug molecules, cisplatin, carboplatin, and oxaliplatin, were investigated using DFT [6]. Calculated geometries of the complexes are in agreement with their available X-ray data.

In many publications, applicability of DFT methods for characterizing the structure of novel platinum complexes with potential antitumor activity was described. Oziminski et al. [7] have calculated the structure and the vibrational and NMR spectra of new Pt(II) and Pt(IV) complexes with histamine and iodohistamine with more than 20 DFT functionals with different basis sets. They compared the results with the experimental data. Juxtapositioning between the X-ray and theoretical geometrical parameters of the [Pt(Hist)Cl₂] complex, it was found that the MPW1PW91, OPW91, and SVWN5 functionals combined with the 6-311G** basis set for nonmetallic and Stuttgart SDD(ECP) basis set for platinum yield the most satisfactory agreement.

Giese et al. [8] have calculated the Raman spectra of some new platinum complexes with pyridine and imidazole derivatives and compared them with the experimental results from normal Raman spectroscopy and surface-enhanced Raman spectroscopy. The authors showed that DFT calculations at the B3LYP/LAN2DZ level can be very useful in the interpretation of experimental spectra of small- and medium-sized systems [8].

Three new Pt(II) compounds with the general formula *cis*-[PtL₂X₂] (where L is 5-methyl-5(4-pyridyl)-hydantoin and X = Cl⁻, Br⁻, I⁻) were recently synthesized and tested for cytotoxic activity on a panel of
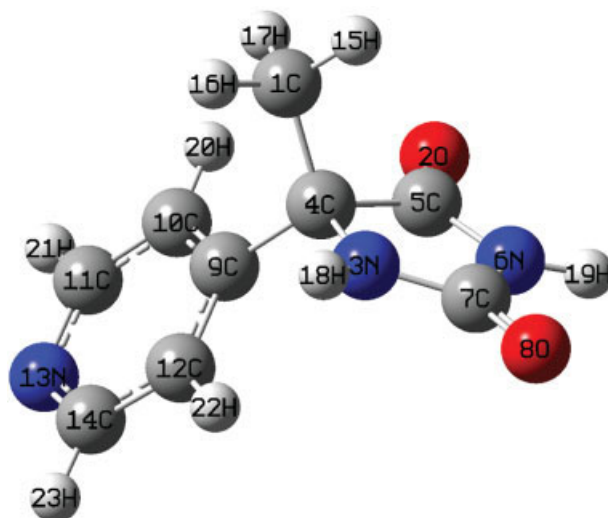

FIGURE 1. Optimized geometry for *R*-5-methyl-5(4-pyridyl)hydantoin. [Color figure can be viewed in the online issue, which is available at www.interscience.wiley.com.]

human tumor cell lines [9]. The aim of this work was to theoretically study the structure and spectroscopic behavior of the new complexes and to calculate some physicochemical parameters for further QSAR investigation of group of similar compounds.

Methods

EXPERIMENTAL

5-Methyl-5(4-pyridyl)hydantoin and its Pt(II) complexes were synthesized, according to Ref. [9].

Infrared (IR) spectra were recorded on IFS 113 v Bruker FTIR spectrophotometer in the range of 4,000–400 cm⁻¹ and 400–150 cm⁻¹ as tablets CsI. Raman spectra were recorded using a Perkin–Elmer Spectrum 2000 NIR FT-Raman with an Nd: YAG 1,064 nm laser. The samples were in solid states.

THEORETICAL

All the calculations were performed on Horseshoe computer cluster (University of Southern Denmark) by Gaussian 03 program, with a combination of Gauss View and GaussSum visualization programs [10].

The hybrid method B3LYP was used with combination of LANL2DZ basis set for all kind of calculations. These calculations include the optimiza-

TABLE I _____

Selected calculated structural parameters of *R*-5-methyl-5(4-pyridyl)hydantoin in comparison with the available experimental data.

	Calculated (LANL2DZ)	Experimental
Bond lengths (Å)		
C1—C4	1.551	1.539 [14]; 1.554 [16]; 1.532 [17]
C4—C5	1.563	1.550 [14]; 1.521 [15]; 1.516 [16]; 1.524 [17]
C5—O2	1.241	1.204 [14]; 1.217 [15]; 1.213 [16]; 1.218 [17]
C5—N6	1.387	1.361 [14]; 1.357 [15]; 1.348 [16]; 1.376 [17]
C7—N6	1.423	1.417 [14]; 1.408 [15]; 1.371 [16]; 1.395 [17]
C7—O8	1.241	1.209 [14]; 1.212 [15]; 1.216 [16]; 1.211 [17]
C7—N3	1.382	1.332 [14]; 1.336 [15]; 1.345 [16]; 1.352 [17]
N3—H18	1.010	0.860 [14]; 0.838 [15]; 0.566 [16]
C4—N3	1.473	1.465 [14]; 1.465 [15]; 1.456 [16]; 1.467 [17]
C4—C9	1.539	1.529 [14]; 1.519 [16]; 1.515 [17]; 1.509 [22]
C9—C10	1.412	1.395 [19]; 1.387 [21]; 1.402 [22]
C10—H20	1.085	0.930 [19]; 0.930 [21]; 0.951 [22]
C10—C11	1.405	1.371 [19]; 1.385 [21]; 1.380 [22]
C11—N13	1.359	1.339 [18]; 1.328 [19]; 1.351 [20]; 1.334 [21]; 1.359 [22]
C14—N13	1.355	1.338 [18]; 1.328 [19]; 1.349 [20]; 1.332 [21]; 1.357 [22]
Angles (°)		
C4—C5—N6	110.34	107.17 [14]; 107.50 [15]; 107.27 [16]
C4—C5—O2	126.36	127.20 [14]; 125.53 [15]; 125.15 [16]
C5—N6—C7	113.24	112.64 [14]; 112.52 [15]; 112.65 [16]
N6—C7—N3	105.41	106.06 [14]; 105.74 [15]; 106.75 [16]
C4—N3—C7	114.18	113.84 [14]; 113.02 [15]; 112.96 [16]
C4—N3—H18	124.33	123.08 [14]; 123.49 [15]; 121.93 [16]
C10—C9—C12	117.72	117.65 [18]; 115.77 [19]; 117.96 [20]; 117.57 [21]; 117.01 [22]
C9—C10—C11	119.11	119.49 [18]; 119.30 [19]; 118.63 [20]; 118.86 [21]; 120.01 [22]
C10—C11—N13	123.45	121.43 [18]; 125.79 [19]; 122.88 [20]; 124.23 [21]; 122.60 [22]
C11—N13—C14	117.15	119.78 [18]; 114.02 [19]; 117.87 [20]; 116.14 [21]; 117.46 [22]
H21—C11—N13	115.93	117.13 [19]; 118.59 [20]; 117.88 [21]; 118.64 [22]
N13—C14—H23	116.06	117.13 [19]; 118.81 [20]; 117.94 [21]; 118.68 [22]
C10—C11—H21	120.61	117.08 [19]; 118.88 [20]; 117.83 [21]; 118.72 [22]

tion of the geometry at three levels of energy convergence in order to find the global minimum. The calculations of the charge distribution was carried out based on the electrostatic potential and NBO analysis, IR, and Raman spectra. Only real harmonic vibrational frequencies for the ligand and the three Pt complexes were found.

The hybrid DFT method (B3LYP [11–13]) was used because of its high accuracy and it is not computationally demanding when it is applied for [Pt(5-methyl-5(4-pyridyl)-2,4-imidazolidenedione)$_2$(halogeno)$_2$] complexes (up to 60 atoms). The basis set LANL2DZ was chosen to include the pseudopotential of the core electrons in atoms of heavy elements like platinum and it is compatible with all other organic elements (C, N, H, O, Hal).

Results and Discussion

STRUCTURE

Because no crystal structure data were yet reported on 5-methyl-5(4-pyridyl)hydantoin, we optimized its structure and the structure of its new platinum complexes. Then we compared them with the literature data for other 5,5'-disubstituted hydantoins, pyridine derivatives, and their platinum complexes [14–30].

The fully optimized structure of 5-methyl-5(4-pyridyl)hydantoin is shown in Figure 1. The calculated structural parameters as bond lengths and angles in comparison with the literature data are

listed in Table I. (The labeling of the atoms is shown in Fig. 1.)

There is good correlation between calculated values of bond lengths and angles and the experimental data for other similar compounds. The calculated bond lengths in the hydantoin ring are very close to these, obtained for Pt(II) complex of 3-amino-5-methyl-5-phenylhydantoin [14]. The theoretical values are a little bit higher than that obtained from the X-ray data for our complex and other known hydantoins. The calculated angles in the pyridine ring are about $120° \pm 3°$, which confirms its planar structure. The fully optimized structures of the three cis-complexes with their labeled atoms are presented in Figures 2–4. Some selected calculated structural parameters in comparison with the literature data are listed in Table II.

The calculated bond lengths of the organic molecules have the same values for the three complexes, which are close to those calculated for the free organic ligand. The theoretical angles in the pyridine and the hydantoin rings are similar to the crystal structures of known compounds. The Pt—N bond lengths weakly decrease in the order $PtL_2I_2 > PtL_2Br_2 > PtL_2Cl_2$, correlating well with the experimental data for similar compounds. From the obtained results of the optimization procedure for all the complexes it can be concluded that the geometries of $N_{Py}Pt(X)_2N_{Py}$ are plane square. All the angle sizes in that area are close to 90° or 180°, depending on their position.

VIBRATIONAL SPECTRA

IR and Raman spectra of the new platinum complexes were calculated. The data on vibration fre-
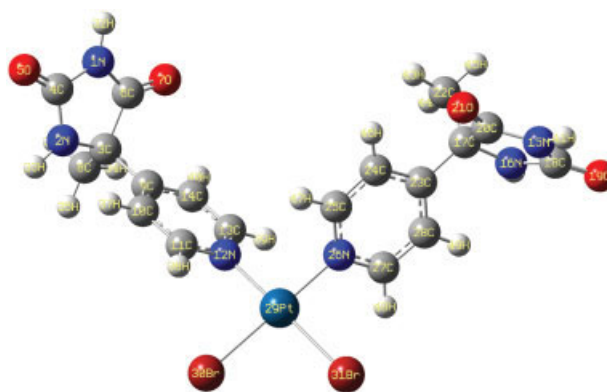
FIGURE 3. Optimized geometry for the complex cis-[PtL_2Br_2]. [Color figure can be viewed in the online issue, which is available at www.interscience.wiley.com.]

quencies must be scaled by factor, because the theoretical vibrations are harmonic and the experimental ones are anharmonic. This factor has specific value for each method—for DFT methods it is 0.98. Some of the characteristic IR frequencies for the complexes are compared with the calculated ones in Table III. Chosen frequencies from the Raman spectra are compared in Table IV. The vibration assignment is in accordance with the literature data.

Vibrations in the Hydantoin Ring

In the experimental IR spectra for the stretching vibrations ν(N—H) we can observe a broad band between 3,600 and 3,100 cm^{-1} for all the complexes. Their corresponding theoretical spectra are presented by four peaks between 3,677 and 3,662 cm^{-1}(unscaled values). The difference in the results

FIGURE 2. Optimized geometry for the complex cis-[PtL_2Cl_2]. [Color figure can be viewed in the online issue, which is available at www.interscience.wiley.com.]

FIGURE 4. Optimized geometry for the complex cis-[PtL_2I_2]. [Color figure can be viewed in the online issue, which is available at www.interscience.wiley.com.]

TABLE II
_____

Selected calculated structural parameters of _cis_-[PtL$_2$Cl$_2$], _cis_-[PtL$_2$Br$_2$], and _cis_-[PtL$_2$I$_2$] in comparison with available experimental data.

| | | Calculated (LAN2DZ) | | |
	Experimental	[PtL$_2$Cl$_2$]	[PtL$_2$Br$_2$]	[PtL$_2$I$_2$]
Bond lengths (Å)				
C3—N2	1.465 [14]; 1.465 [15]; 1.456 [16]; 1.467 [17]	1.472	1.472	1.472
N2—C4	1.332 [14]; 1.336 [15]; 1.345 [16]; 1.352 [17]	1.385	1.385	1.385
C4—O5	1.209 [14]; 1.212 [15]; 1.216 [16]; 1.211 [17]	1.240	1.240	1.240
C4—N1	1.417 [14]; 1.408 [15]; 1.371 [16]; 1.395 [17]	1.426	1.426	1.426
C6—C3	1.550 [14]; 1.521 [15]; 1.516 [16]; 1.524 [17]	1.565	1.565	1.565
C3—C9	1.529 [14]; 1.519 [16]; 1.515 [17]; 1.509 [22]	1.536	1.536	1.536
C9—C10	1.395 [19]; 1.387 [21]; 1.402 [22]	1.407	1.407	1.407
C11—N12	1.339 [18]; 1.328 [19]; 1.351 [20]; 1.334 [21]; 1.359 [22]	1.364	1.363	1.363
C13—N12	1.338 [18]; 1.328 [19]; 1.349 [20]; 1.332 [21]; 1.357 [22]	1.366	1.365	1.364
Pt29—N26	2.026 [20]; 2.020 [21]; 2.046 [24]; 2.04 [25]; 2.039 [26]; 2.052 [26]; 2.060 [26]; 2.112 [30]	2.061	2.073	2.091
Pt29—N12	2.026 [20]; 2.02 [23]; 1.994 [24]; 2.01 [25]; 2.027 [26]; 2.037 [26]; 2.056 [26]; 2.113 [30]	2.057	2.071	2.090
Pt29—Cl30	2.291 [23]; 2.309 [24]; 2.300 [25]; 2.306 [26]	2.404	—	—
Pt29—Cl31	2.289 [23]; 2.298 [24]; 2.291 [25]; 2.304 [26]	2.403	—	—
Pt29—Br30	2.446 [28]; 2.495 [29]	—	2.541	—
Pt29—Br31	2.441 [28]; 2.486 [29]	—	2.539	—
Pt29—I30	2.610 [20]; 2.578 [26]; 2.590 [26]; 2.593 [30]; 2.595 [30]; 2.604 [30]	—	—	2.694
Pt29—I31	2.610 [20]; 2.602 [26]; 2.598 [26]; 2.597 [30]; 2.596 [30]; 2.604 [30]	—	—	2.691
Angles (°)				
C6—N1—C4	112.64 [14]; 112.52 [15]; 112.65 [16]	113.30	113.31	113.31
N1—C4—N2	106.06 [14]; 105.74 [15]; 106.75 [16]	105.40	105.40	105.40
C4—N2—C3	113.84 [14]; 113.02 [15]; 112.96 [16]	114.02	114.01	114.01
C10—C9—C14	117.65 [18]; 115.77 [19]; 117.96 [20]; 117.57 [21]; 117.01 [22]	117.63	117.65	117.66
C9—C10—C11	119.49 [18]; 119.30 [19]; 118.63 [20]; 118.86 [21]; 120.01 [22]	120.10	120.03	119.93
C10—C11—N12	121.43 [18]; 125.79 [19]; 122.88 [20]; 124.23 [21]; 122.60 [22]	121.73	121.80	121.91
C11—N12—C13	119.78 [18]; 114.02 [19]; 117.87 [20]; 116.14 [21]; 117.46 [22]	118.64	118.63	118.58
Pt29—N26—C27		120.37	120.85	121.18
Pt29—N26—C25		121.06	120.60	120.30
N12—Pt29—N26	91.20 [23]; 91.26 [24]	92.89	91.66	90.18
Cl30—Pt29—Cl31	91.60 [23]	91.64	—	—
N26—Pt29—Cl31		88.21	—	—
N12—Pt29—Cl30		87.27	—	—
N26—Pt29—Cl30		179.31	—	—
Br30—Pt29—Br31	87.02 [28]; 88.12 [29]	—	91.30	—
N26—Pt29—Br31		—	88.90	—
N12—Pt29—Br30		—	88.14	—
N26—Pt29—Br30		—	179.59	—
I30—Pt29—I31		—	—	90.18
N26—Pt29—I31		—	—	89.53
N12—Pt29—I30		—	—	88.84
N26—Pt29—I30		—	—	179.00

TABLE III
Theoretical and experimental data of IR spectra of the complexes.

cis-PtL$_2$Cl$_2$				Cis-PtL$_2$Br$_2$				cis-PtL$_2$I$_2$				Vibr. assignment
B3LYP freq.	Int.	B3LYP scaled	Exp. freq.	B3LYP freq.	Int.	B3LYP scaled	Exp. freq.	B3LYP freq.	Int.	B3LYP scaled	Exp. freq.	
3,676.6	105.2	3,603.1	3,351.0br	3,673.6	46.0	3,600.2	3,842.0br	3,677.0	45.3	3,603.5	3,224.4br	ν(N—H)
3,672.9	124.5	3,599.4		4,673.0	48.8	4,579.5		3,673.0	45.5	3,599.5		
3,662.4	49.7	3,589.1		3,662.5	123.9	3,589.3		3,662.5	115.2	3,589.3		
3,662.3	49.4	3,589.0		3,662.1	115.6	3,588.9		3,662.3	114.5	3,589.1		
1,771.7	183.4	1,736.3	1,777.2m	1,771.7	204.6	1,736.2	1,777.2m	1,771.5	220.2	1,736.0	1,762.0m	ν(C=O)
1,770.7	812	1,735.3		1,770.7	787.0	1,735.3		1,770.6	769.5	1,735.1		
1,730.1	184.3	1,695.5	1,725.5s	1,730.4	598.0	1,695.8	1,724.8s	1,730.4	658.9	1,695.8	1,724.4s	
1,728.5	716.5	1,693.9		1,728.4	694.9	1,693.8		1,728.4	585.7	1,693.8		
1,657.5	32.8	1,624.4	1,619.9w	1,655.8	34.8	1,622.7	1,618.4w	1,653.9	36.6	1,620.8	1,615.2w	δ(C—H); ν(C=C)-pyr
1,656.8	19.6	1,623.7		1,654.9	24.5	1,621.8		1,652.7	29.8	1,619.6		
1,460.9	20.1	1,431.6	1,427.08m	1,458.9	13.3	1,429.7	1,425.8m	1,456.6	30.8	1,427.5	1,424.4m	δ(C—H)-pyr
1,460.2	19.6	1,431.0		1,458.3	69.7	1,429.1		1,455.8	52.9	1,426.6		
1,349.1	386.8	1,322.1	1,402.9m	1,349.0	356.3	1,322.1	1,405.4m	1,349.0	341.8	1,322.1	1,378.3sh	δ(C—N)-hyd
1,348.4	185.8	1,321.5		1,348.5	199.8	1,321.5		1,348.7	214.9	1,321.7		
1,279.1	10.1	1,253.5	1,261w	1,278.5	18.0	1,252.9	1,260.5w	1,277.3	47.8	1,251.8	1,262.1w	δ(C—H)-pyr
1,278.0	7.7	1,252.4		1,277.3	191.5	1,251.8		1,275.8	172.7	1,250.3		
530.3	142.1	519.7	509.1w	529.3	146.9	518.7	518.9w	530.6	152.3	520.0	520.8w	δ(N—H)-hyd
519.8	121.5	509.4		518.1	124.5	507.7		517.2	131.3	506.9		
331.8	19.4	325.2	329.9m									ν(Pt—Cl)
328.4	13.6	321.9	322.6sh									
				220.9	8.5	216.5	235.4w					ν(Pt—Br)
				217.5	9.0	213.2	235.2w					
								193.2	1.5	189.3	189.0w	ν(N—Pt—I)—

Freq., frequencies; int., intensities; br, broad; m, medium; s, strong; w, weak; sh, shoulder.

TABLE IV
Theoretical and experimental data of Raman spectra of the complexes.

cis-PtL₂Cl₂				cis-PtL₂Br₂				cis-PtL₂I₂				Vibr. assignment
B3LYP freq.	Int.	B3LYP scaled	Exp. freq.	B3LYP freq.	Int.	B3LYP scaled	Exp. freq.	B3LYP freq.	Int.	B3LYP scaled	Exp. freq.	
3,172	42.3	3,109	3,084(29)	3,172	43.5	3,108	3,076(30)	3,174	43.0	3,110	3,076(34)	νC—H(CH₃)
3,172	43.1	3,108		3,171	44.9	3,108		3,172	45.1	3,108		
3,157	94.1	3,093	2,992(19)	3,157	95.8	3,094	2,987(22)	3,157	98.5	3,094	3,057(30)	
3,154	90.2	3,091		3,154	91.4	3,091		3,154	94.2	3,091		
3,061	162.3	3,000	2,942(22)	3,061	163.7	3,000	2,929(16)	3,062	165.8	3,001	2,980(23)	
3,060	152.4	2,998		3,059	153.7	2,998		3,060	159.8	2,998		
1,770	68.9	1,735	1,769(33)	1,778	81.6	1,742	1,771(28)	1,772	84.7	1,736	1,768(39)	ν(C=O)-hyd
1,769	4.8	1,734		1,771	16.6	1,735		1,771	21.0	1,735		
1,658	457.1	1,624	1,621(97)	1,656	453.5	1,623	1,619(91)	1,654	465.2	1,621	1,613(73)	δ(C—H); ν(C=C)-pyr
1,657	396.4	1,624		1,655	415.4	1,622		1,653	426.7	1,620		
1,255	85.9	1,230	1,219(44)	1,254	101.6	1,229	1,216(43)	1,254	115.2	1,229	1,216(75)	δ(C—H)-pyr
1,255	55.0	1,230		1,253	73.1	1,228		1,253	85.2	1,228		
1,056	343.9	1,034	1,064(98)	1,053	346.1	1,032	1,064(100)	1,083	67.5	1,061	1,058(77)	ν(Pt—N) + δ(C—H)-pyr
1,050	221.7	1,029	1,047(58)	1,046	256.5	1,025	1,045(60)	1,049	351.2	1,028	1,039(79)	
332	9.4	325	332(59)	—	—	—	—	—	—	—	—	ν(Pt—Cl)
328	14.3	322		—	—	—	—	193	11.8	189	189(70)	ν(N—Pt—I)

Freq., frequencies; int., intensities. The intensities of the experimental spectra are given in parentheses.
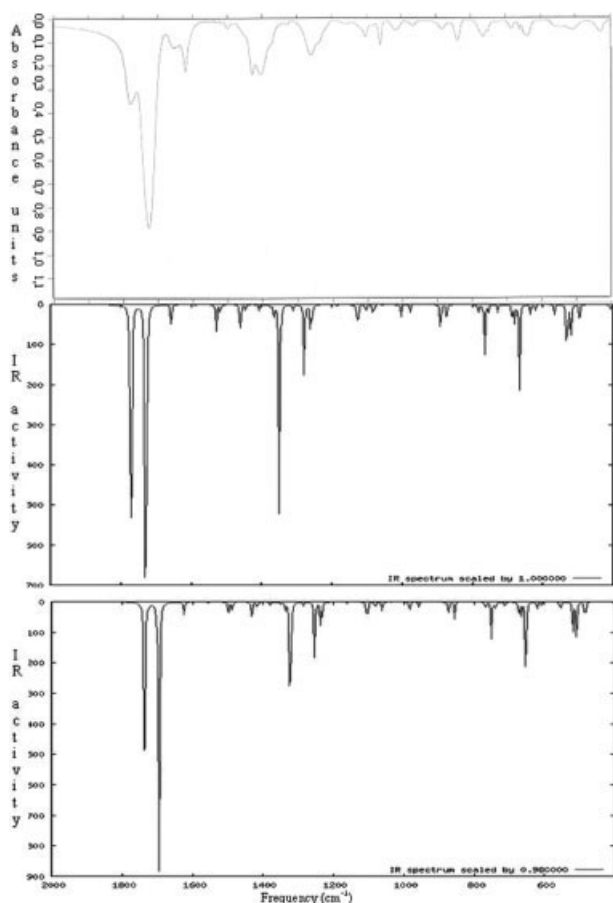
FIGURE 5. Comparison between the experimental (top) and the calculated IR spectra (unscaled in the center and scaled by a factor value of 0.98 on the bottom) of cis-[PtL$_2$Cl$_2$].

is probably because of some inter- and intramolecular interactions like H-bonds between the NH-groups. DFT methods had very low capability to describe hydrogen bonding. The absorption bands for ν(N—H) were not well observed in the experimental Raman spectra.

The different CH$_3$ vibrations are presented by weak peak around 2,770 cm^{-1} in the experimental IR spectra for the three complexes. The same vibrations can be well observed in the Raman spectra and they are well predicted in the calculations (see Table IV).

ν(C=O) vibrations are well forecasted in both IR and Raman spectra without scaling the theoretical results. The absorption bands in the IR spectra are much stronger than those in the Raman spectra. There is good agreement between the experimental and scaled theoretical frequencies for δ(N—H) around 520 and 509 cm^{-1}.

The experimental spectra of cis-[PtL$_2$Cl$_2$] in comparison with the calculated spectra ranged 2,000–400 cm^{-1} and are shown in Figure 5.

Vibrations of the Pyridine Ring

Assignment of the pyridine ring vibrations gave important information for the mode of coordination of the organic ligand with platinum ion, which is namely through the pyridine nitrogen. This can be well observed from the comparative analysis of the IR spectra of the three complexes and the free ligand. δ(C—H) and ν(C=C) in the pyridine ring were at 1,619.9, 1,618.4, and 1,615.2 cm^{-1} for the chloro-, bromo-, and iodo-complexes, respectively, which differs from 1,605.3 cm^{-1} in the free ligand. Vibrations of δ(C—H) in the pyridine ring could be observed at about 1,426 and 1,261 cm^{-1} for all complexes.

There was good correlation between the experimental data and the scaled theoretical IR frequencies for vibrations in the pyridine ring.

In the Raman spectra, high peaks at 1,621, 1,619, and 1,613 cm^{-1} for the three complexes, respectively, correlated with the scaled theoretical spectra, assigned for δ(C—H) and ν(C=C) in the pyridine ring. The strong peaks between 1,064 and 1,037 cm^{-1} for the three compounds seemed to be the theoretical ν(Pt—N) and δ(C—H) in the pyridine ring.

Vibrations in the Area Under 400 cm^{-1}

Characteristic for cis-[PtL$_2$Cl$_2$] were the stretching asymmetric vibrations Cl—Pt—Cl at 318.2 cm^{-1} and the stretching symmetric vibrations Cl—Pt—Cl at 331.8 cm^{-1}. These were the unscaled calculated values, which showed higher intensities in the IR then in the Raman spectra. The corresponding experimental results in IR spectra were at 329.9 and 322.6 cm^{-1} (shoulder). The peak at 332 cm^{-1} in the experimental Raman spectra most probably corresponds to the theoretical peak at 328.4 cm^{-1} for N$_{py}$—Pt—Cl vibrations.

The stretching vibrations Br—Pt—Br for the complex cis-[PtL$_2$Br$_2$] were at 220.9 and 217.4 cm^{-1} in the theoretical spectra, which correspond to the peaks at 235.2 and 232.4 cm^{-1} in the experimental IR spectra and at 233 and 205 cm^{-1} in the experimental Raman spectra. The extraplanar Pt—N$_{py}$ vibrations (374.6, 371.1, 323.6, 317.7 cm^{-1} – unscaled values) can be seen in the experimental spectra—373 and 321 cm^{-1} in the Raman and 328 cm^{-1} in the IR spectra.
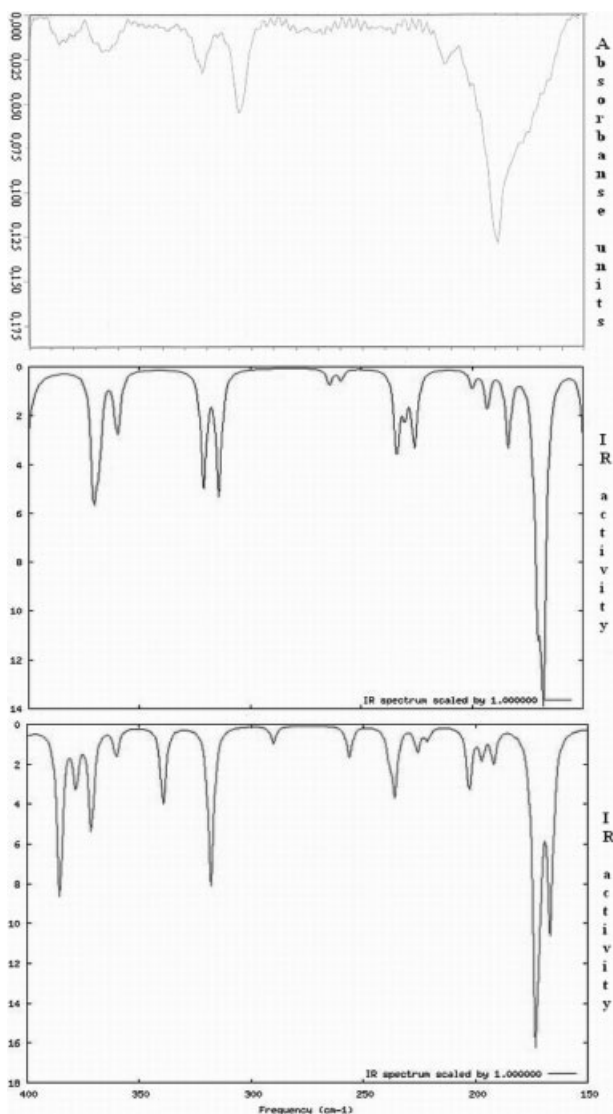
FIGURE 6. Comparison between experimental IR spectra of [PtL$_2$I$_2$] (top) and the calculated IR spectra for cis-[PtL$_2$I$_2$] (center) and for trans-[PtL$_2$I$_2$] (bottom).

In a previous publication [9] we presumed the trans-geometry of [PtL$_2$I$_2$]. According to other experiments such as the Kurnakov test [31] and Raman spectra, most probably, the new complex is cis-[PtL$_2$I$_2$], which is logical from its way of synthesis [32] and the concept of the trans-effect [33]. However, isomerization can occur during the synthesis [30], and trans-[PtL$_2$I$_2$] is also formed because the experimental and theoretical IR and Raman spectra were similar. On the basis of the obtained results the solid compound is most likely a mixture of both of these isomers. Trans-iodine complex seemed to be more stable, because of its single-

point energy ($-1,468.116425$ a.u.), compared with the energy of its cis-isomer ($-1,468.092515$ a.u.). The energy difference between trans- and cis-isomers is around 63 kJ/mol. The scheme of the calculated IR spectra for cis- and trans-[PtL$_2$I$_2$] and the experimental spectra of the complex in the range $400-150$ cm^{-1} is given in Figure 6.

The calculated bands with low intensities in the IR spectra at 193.2 and 183.6 cm^{-1} (unscaled values) for N—Pt—I vibrations most probably corresponded to the experimental peak at 189.0 cm^{-1} and its shoulder at 176.5 cm^{-1}.

The highest peak in the range under 400 cm^{-1} in the experimental Raman spectra was at 189 cm^{-1}. Most probably, it corresponded to the peak at 193.2 cm^{-1} (189.3 scaled) from the calculated spectra, which was assigned for N—Pt—I vibrations.

The extraplanar pyridine vibrations and other skeletal vibrations were calculated at 403.7 (395.6), 370.7 (363.3), 368.4 (361.0), 321.1 (314.7), and 314.3 (308.1) cm^{-1}, which corresponded to 386.7, 367.2, 322.1, and 305.4 cm^{-1} in the experimental IR spectra (the values in parentheses are scaled with a factor value of 0.98).

CHARGES

The distribution of the charge in the complexes was calculated on the basis of the electrostatic potential. The results are listed in Table V.

In all the complexes, positive charge of both nitrogen atoms and negative charge of platinum atom were observed. These facts are proofs for typical coordinative bonds between pyridine nitrogen atoms and platinum atom. Large electronegativity of chlorine and bromine atoms also contributes for withdrawal of electronic density from nitrogen atom through platinum atom to the halogen atom and for decreasing of the charge of nitrogen atom.

TABLE V

Selected values of ESP charges of the three complexes, compared with the free ligand.

	ESP charge				
Complex	q (N-pyr)1	q (N-pyr)2	q (Pt)	q (X1)	q (X2)
L		-0.642	—	—	—
PtL$_2$Cl$_2$	0.116	0.183	-0.218	-0.338	-0.349
PtL$_2$Br$_2$	0.241	0.293	-0.405	-0.288	-0.304
PtL$_2$I$_2$	0.241	0.264	-0.472	-0.241	-0.246

TABLE VI

Occupancy of natural bond orbital (NBOs) and hybrids calculated for *cis*-[PtL$_2$Cl$_2$].

Donor Lewis-type NBOs (A—B) bond	Occupancy	Hybrid	AO %	Acceptor-type non-Lewis NBOs	NBOs
σ(Pt—Cl)	1.964	sd (Pt)	s (46.34%), p (0.31%), d (53.35%)	σ^*(Pt—Cl)	0.33
σ(Pt—Cl)	1.964	p (Cl)	s (9.97%), p (90.03%)		
LP(N12)	1.685	sp^3	s (25.98%), p (74.02%)	Ry(1) Pt	0.02
LP(N26)	1.680	sp^3	s (26.03%), p (73.97%)	Ry(2) Pt	0.004
LP(N15)	1.645	p	s (0.01%), p (99.99%)	Ry(3) Pt	0.003
LP1(O5)	1.978	sp0.5	s (64.81%), p (35.19%)	Ry(4) Pt	0.003
LP2(O5)	1.850	p	s (0.00%), p (100.00%)	Ry(5) Pt	0.002
LP1(O19)	1.977	sp0.6	s (64.67%), p (35.33%)	Ry(6) Pt	0.002
LP2(O19)	1.850	sp	s (0.00%), p (100.00%)	Ry(7) Pt	0.001

NBO ANALYSIS OF *cis*-[PtL$_2$Cl$_2$]

This NBO analysis supports the results based on NBO charges for the absence of coordination bond between pyridine nitrogen and platinum atom. If we judge on the occupancy, lone electron pair belongs mainly to the pyridine nitrogen atom. For platinum atom there are only Rydberg orbitals, which are weakly populated. The biggest probability for the formation of donor–acceptor type of bonding is Pt with pyridine nitrogen in comparison to other nitrogen or oxygen atoms. The reason for this is the highest population of Rydberg Pt orbital, corresponding to the pyridine nitrogen atom.

The bond Pt—Cl is formed by sd hybrid orbital of platinum atom and p-orbital of chlorine atom.

The results from the NBO analysis are listed in Table VI.

CALCULATION OF OTHER PHYSICOCHEMICAL PROPERTIES

Other physicochemical constants, such as dipole moments and energy of HOMO and LUMO, were calculated and listed in Table VII.

TABLE VII

Some physicochemical properties of the complexes, compared with the free ligand.

Compound	μ (D)	E(HOMO) (eV)	E(LUMO) (eV)
L	2.90	−7.10	−1.61
PtL$_2$Cl$_2$	13.35	−6.06	−2.62
PtL$_2$Br$_2$	13.35	−5.78	−2.62
PtL$_2$I$_2$	13.04	−5.68	−2.42

From the calculated physicochemical parameters it can be seen that these platinum complexes are extremely polar compounds. They have much bigger dipole moment than the ligand. The Pt complexes have lower redox potential (3.0–3.4 eV), in comparison to the ligand, which has HOMO/LUMO gap around 5.5 eV. The lower energy of HOMO (negative) and the negative values of LUMO show that these molecules have the properties of reductors.

These constants can be used as descriptors for further QSAR analysis of series of metal complexes of this type.

Conclusions

The geometry of 5-methyl-5-(4-pyridyl)hydantoin and its new Pt(II) complexes were optimized, using the hybrid DFT method B3LYP with LANL2DZ basis set. This method gave good results, comparable with the experimental data from the literature for similar compounds.

The metal–ligand binding mode in the new complexes was confirmed from the calculations. In all the complexes, platinum coordinates monodentate manner through the pyridine nitrogen atom.

B3LYP/LANL2DZ was also used for predicting IR and Raman spectra for the new compounds. The calculations helped in the explanation of the vibrational behavior of the platinum complexes. The comparison with the experimental data showed that using a scaling factor of 0.98 is not suitable for all the predicted frequencies in the IR and Raman spectra.

References

1. Rosenberg, B.; VanCamp, L. Nature 1965, 205, 698.

2. Momekov, G.; Momekova, D. Expert Opin Ther Patents 2006, 16, 1383.

3. Wysokinsky, R.; Michalska, D. J Comput Chem 2001, 22, 901.

4. Amado, A.; Fiuza, S.; Marques, M.; de Carvalho, L. B. J Chem Phys 2007, 127, 185104.

5. Wisokyinsky, R.; Jaworska, J.; Michalska, D. J Mol Struct (Theochem) 2006, 758, 169.

6. Sarmah, P.; Deka, R. Int J Quantum Chem 2008, 108, 1400.

7. Oziminski, W.; Garnuszek, P.; Bednarek, E.; Dobrowolski, J. Inorg Chim Acta 2007, 360, 1902.

8. Giese, B.; Deacon, G.; Jaworska, J.; McNaughton, D. Biopolymers (Biospectroscopy) 2002, 67, 294.

9. Bakalova, A.; Varbanov, H.; Buyukliev, R.; Momekov, G.; Ferdinandov, D.; Konstantinov, S.; Ivanov, D. Eur J Med Chem 2008, 43, 958.

10. Frisch, M.; Trucks, G.; Schlegel, H.; Scuseria, G.; Robb, M.; Cheeseman, J.; Montgomery, J.; Vreven, T.; Kudin, K.; Burant, J.; Millam, J.; Iyengar, S.; Tomasi, J.; Barone, V.; Mennucci, B.; Cossi, M.; Scalmani, G.; Rega, N.; Petersson, G.; Nakatsuji, H.; Hada, M.; Ehara, M.; Toyota, K.; Fukuda, R.; Hasegawa, J.; Ishida, M.; Nakajima, T.; Honda, Y.; Kitao, O.; Nakai, H.; Klene, M.; Li, X.; Knox, J.; Hratchian, H.; Cross, J.; Bakken, V.; Adamo, C.; Jaramillo, J.; Gomperts, R.; Stratmann, R.; Yazyev, O.; Austin, A.; Cammi, R.; Pomelli, C.; Ochterski, J.; Ayala, P.; Morokuma, K.; Voth, G.; Salvador, P.; Dannenberg, J.; Zakrzewski, V.; Dapprich, S.; Daniels, A. D.; Strain, M.; Farkas, O.; Malick, D.; Rabuck, A.; Raghavachari, K.; Foresman, J. B.; Ortiz, J.; Cui, Q.; Baboul, A.; Clifford, S.; Cioslowski, J.; Stefanov, B.; Liu, G.; Liashenko, A.; Piskorz, P.; Komaromi, I.; Martin, R.; Fox, D.; Keith, T.; Al-Laham, M.; Peng, C.; Nanayakkara, A.; Challacombe, M.; Gill, P.; Johnson, B.; Chen, W.; Wong, M.; Gonzalez, C.; Pople, J. Gaussian 03. Program for quantum chemistry; Carnegie Mellon University: Pennsylvania.

11. Becke, A. Phys Rev A 1988, 38, 3098.

12. Becke, A. J Chem Phys 1992, 96, 2155.

13. Lee, C.; Yang, W.; Parr, R. Phys Rev A 1988, 37, 785.

14. Bakalova, A.; Petrova, R.; Shivachev, B.; Varbanov, H. J Coord Chem 2007, 60, 1701.

15. Shivachev, B.; Petrova, R.; Naydenova, E. Acta Cryst 2005, C61, o524.

16. Coquerel, G.; Petit, M.; Robert, F. Acta Cryst 1993, C49, 824.

17. Lisagarten, J. N.; Palmer, A. Acta Cryst 1980, B36, 2345.

18. Rowan, K. R.; Holt, E. M. Acta Cryst 1995, C51, 2554.

19. Ni, J.; Li, Y.-Z.; Qi, W.-B.; Liu, Y.-J.; Chen, H.-L.; Wang, Z.-L. Acta Cryst 2003, C59, 470.

20. Tessier, C.; Rochon, F. Acta Cryst 2006, C62, m620.

21. He, M.-Y.; Chen S.-C.; Chen, Q. Acta Cryst 2006, E62, 3716.

22. Hensen, K.; Mayr-Stein, R.; Spangenberg, B.; Bolte, M. Acta Cryst 2000, C56, 610.

23. Sakai, K.; Tomita, Y.; Ue, T.; Goshima, K.; Masanatsu, O.; Tsubomura, T.; Matsumoto, K.; Ohmura, K.; Kawakami, K. Inorg Chim Acta 2000, 297, 64.

24. Garnuszek, P.; Maurin, J. K.; Witowska-Jarosz, J.; Ptasiewicz-Bąk, B. Inorg Chim Acta C 2002, 338, 119.

25. Colamarino, P.; Orioli, P. L. J Chem Soc Dalton Trans 1975, 1656.

26. Tessier, C.; Rochon, F. D. Inorg Chim Acta 1999, 295, 25.

27. Thiele, G.; Wagner, D. Chem Ber 1978, 111, 3162.

28. Lövqvist, K. Acta Cryst 1996, C52, 1921.

29. Morgan, J. L.; Robinson, B. H.; Simpson, J. Acta Cryst 2002, E58, 504.

30. Rochon, F. D.; Buculei, V. Inorg Chim Acta 2004, 357, 2218.

31. Kurnakov, N. Himii kompleksni soedinenia. Akad Nauk SSSR 1963, 7.

32. Dhara, S. Indian J Chem 1970, 8, 193.

33. Gel'man, A. D.; Karandashova, E. F.; Essen, L. N. Dokl Akad SSSR 1948, 63, 37.